Chinese J. of Chem. Eng., **9** (4) 436 – 440 (2001)
RESEARCH NOTES

An Investigation on the Void Fraction for upward Gas-Liquid Slug Flow in Vertical Pipe

XIA Guodong(夏国栋)[a,*], ZHOU Fangde(周芳德)[b] and HU Mingsheng(胡明胜)[b]
[a]College of Environmental and Energy Engineering, Beijing Polytechnic University, Beijing 100022, China
[b]State Key Laboratory of Multiphase Flow in Power Engineering, Xi'an Jiaotong University, Xi'an 710049, China

Abstract In order to investigate the influence of the entrance effect on the spatial distribution of phases, the experiments on gas-liquid two-phase slug flow in a vertical pipe of 0.03 m ID were carried out by using optical probes and an EKTAPRO 1000 high speed motion analyzer. It demonstrates that the radial profile of slug flow void fraction is parabolic. Influenced by the falling liquid film, the radial profile curve of liquid slug void fraction in the wake region is also parabolic. Since fully turbulent velocity distribution is built up in the developed region, the void fraction profile in this region is the saddle type. At given superficial liquid velocity, the liquid slug void fraction increases with gas velocity. The radial profiles of liquid slug void fraction at different axial locations are all saddle curves, but void fraction is obviously high around the centerline in the entrance region. The nearer the measuring station is from the entrance, the farther the peak location is away from the wall.
Keywords gas-liquid slug flow, void fraction, vertical pipe

1 INTRODUCTION

Slug flow is a predominant flow pattern for vertical gas-liquid two-phase flow. It is characterized by alternating Taylor bubbles and liquid slugs flowing through the pipeline. In the film around a Taylor bubble, gravity forces the liquid to fall so that it impinges the liquid slug, causing a flow separation at the bubble tail. Under certain conditions small bubbles are entrained into the liquid slug, either coalesced in the front of the following bubble or being carried into the next falling film. To calculate the pressure loss of the flow, the knowledge of the spatial distribution of the gas phase is necessary.[1]

Akagawa[2] made a detailed investigation on vertical air/water slug flow in 27.6 mm diameter pipe using the conductance wires. The experimental data obtained showed that more than 30% of gas existed in the liquid slugs. Mao & Dukler[3] measured the distribution of void fraction for the liquid slugs using a high-precision radio-frequency probe. Lately, Van Hout *et al.*[4] measured the distribution of void fraction in liquid slugs using the optical probes and qualitatively explained the reason that high void fraction turns up in the front of the liquid slugs. Small bubbles are produced due to the tearing from the Taylor bubble tail and dispersed into the liquid slug. The dispersed bubbles are then recaptured by the next Taylor bubble which comes along.

It is noted that the developing slug flow is encountered more frequently in practice. Thus, research on the slug flow including the entrance effect is important. This work reports the experimental investigation on the void fraction for gas-liquid slug flow in a vertical pipe by using the optical probes and the high speed motion analyzer.

2 EXPERIMENTAL SYSTEM AND METHOD

Figure 1 shows the schematic diagram of the experimental system. Water and air are used as working fluids. Their flow rates are measured by the rotameters. These two fluids are allowed to mix in the mixing chamber at the bottom of the pipe. Water enters the mixing chamber in the axial direction through a pipe with the same diameter as the test section. Air is introduced peripherally through uniformly distributed small holes with diameter 2 mm. The length of the mixing chamber is about 0.4 m. The test section is made of a transparent pipe with 0.03 m ID and 6 m long. The measuring stations are installed at the three locations, namely at 0.9, 2.4, 4.5 m above the entrance. The U-type optical probes with 3000—5000 Hz collecting frequency are used to measure the void fraction. The measuring time is 30—60 s so that each value of void fraction is the average of more than 30 slug units. The optical probes are installed in such a way that their radial positions in the pipe can be changed easily. Measurements are taken at eight radial positions in the pipe, namely at $r = 0$, 1.5, 4, 6, 8, 10, 12, 14 mm. The threshold value is obtained in the synchronous measuring way by using the EKTAPRO 1000 high speed motion analyzer and the optical probe

Received 2000-07-07, accepted 2001-04-03.
* To whom correspondence should be addressed.

at the same measuring station. Over five slug units are measured every time. By analyzing the pictures recorded by the high speed motion analyzer, the time for the Taylor bubble i ($i = 1, 2, \cdots, n$) passing by (accurate up to 0.001 s) can be obtained. Therefore, the corresponding threshold values F_i ($i = 1, 2, \cdots, n$) can be gained by comparing to the signals measured by the optical probe. It can refer to their mean value as the threshold value in this flow condition as follows

$$F = \frac{1}{n}\sum_{i=1}^{n} F_i \tag{1}$$

The frame rate of the high-speed motion analyzer is 1000 frames per second. A transparent, water-filled, rectangular box was fitted onto the measuring station(4.5 m) to allow undistorted video-graphic measurements. A scattering back light was used in order to create a nearly back subject (bubbles) on a nearly white background (water). The image frames describing the two-phase flow field were recorded and stored in the special cassettes. In order to obtain the information on slug flow, a series of image analysis steps must be further undertaken. Motion program is a menu-driven software package designed to facilitate the task of digitizing object motion recorded by high-speed video systems. Using the motion program, collecting points, line segments, velocities *etc.* was very simple and the data collected directly were stored in the computer. The error is within 2.8%.

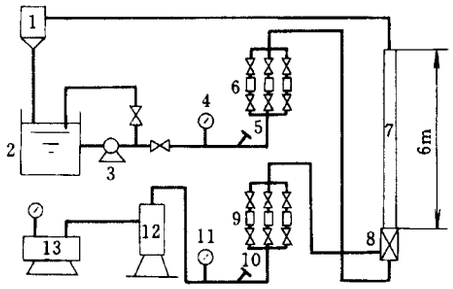

Figure 1 Schematic diagram of the experimental system

1—filter; 2—tank; 3—pump; 4,11—pressure gauge; 5,10—thermometer; 6—water flowmeter; 7—test section; 8—mixing chamber; 9—air flowmeter; 12—stabilizer; 13—air compressor

The experimental conditions are: system pressure 0.1—0.3 MPa, temperature 20—30℃, superficial velocity of water 0.032—1.965 $m \cdot s^{-1}$, superficial velocity of gas 0.1—8.078 $m \cdot s^{-1}$.

3 SLUG UNIT VOID FRACTION

3.1 Radial profiles

Figures 2 and 3 show the radial profiles for slug flow void fraction. The curves present the parabolic shape for a low U_{SL}, and the void fraction increases with the increase of U_{SG}. When U_{SG} is over 6 $m \cdot s^{-1}$, the flow pattern becomes the churn-annular one, and the void fraction values around the centerline approach unity. When the superficial liquid velocity is fairly high, as shown in Fig. 3, two kinds of profiles for the void fraction are observed as the superficial gas velocity changing. One is parabolic, and the other is the saddle profile in the low superficial gas velocity region, which is similar to that of the bubble flow pattern. It indicates that it is the transition from the slug flow to the dispersed bubble flow ($U_{SL} = 0.404\ m \cdot s^{-1}$, $U_{SG} = 1.965\ m \cdot s^{-1}$). The protrusion in the middle of the curve is due to the existence of a few big bubbles under this flow condition.

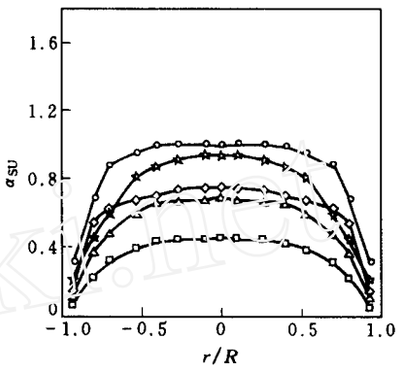

Figure 2 Radial profiles of void fraction for slug unit ($U_{SL} = 0.157\ m \cdot s^{-1}$, $x = 150D$)

U_{SG}, $m \cdot s^{-1}$: □ 0.287; △ 0.742; ◇ 1.196; ☆ 2.902; ○ 8.078

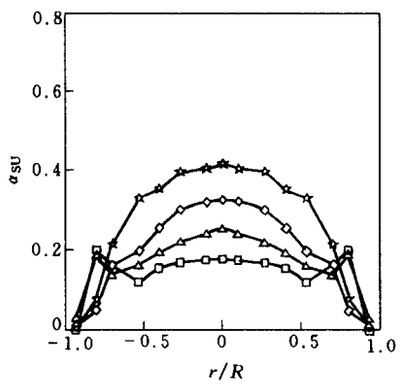

Figure 3 Radial profiles of void fraction for slug unit ($U_{SL} = 1.965\ m \cdot s^{-1}$, $x = 150D$)

U_{SG}, $m \cdot s^{-1}$: □ 0.404; △ 0.670; ◇ 0.848; ☆ 1.178

3.2 Averaged slug unit void fraction

The averaged slug unit void fraction can be calculated by integrating the radial profile. The experimental results of the averaged void fraction are depicted in Fig. 4. When U_{SL} is constant, the averaged void fraction increases with the increase of superficial gas velocity. When the superficial gas velocity is constant, it decreases with increasing superficial liquid velocity.

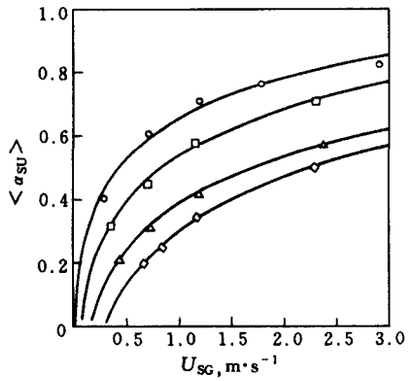

Figure 4 Experimental results of averaged void fraction(x=150D)

U_{SL}, m·s^{-1}: ○ 0.157; □ 0.472; △ 1.179; ◇ 1.965

3.3 Void fraction profiles at different axial positions

In order to research the spatial distribution characteristics of the two phases during the developing process of slug flow, the local void fractions at three axial locations (namely at 30D, 80D and 150D above the entrance) were measured. Fig. 5 represents the void fraction profiles at the different axial locations under a given flow condition. As it can be seen, the void fraction values measured at the entrance (x = 30D) are uniform in the zone of 0—0.7R due to the inlet effect. At the location of x = 80D, the averaged void fraction is slightly less than that of at the entrance. Due the bubble coalescence along with the flow development, the central zone of the curve becomes flat again at the location of x = 150D. One can consider that the slug flow is approximately fully-developed as more than 90% liquid slugs are longer than 0.5L_{stab} at this position[5]. This is in accordance with the analysis presented by Taitel *et al.*[6]: the merging process is very slowly after the length of liquid slug is equal to (or exceed) 0.5L_{stab}.

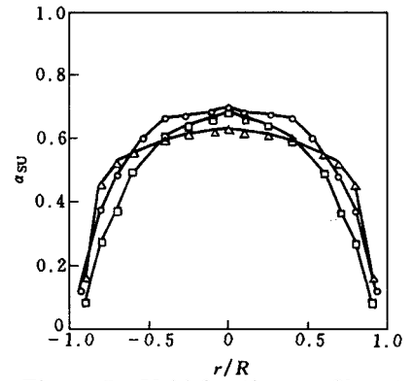

Figure 5 Void fraction profiles at different axial positions

(U_{SG} = 0.742 m·s^{-1}, U_{SL} = 0.157 m·s^{-1})

x: ○ 150D; □ 80D; △ 30D

Among the three locations, the averaged void fraction at x = 80D is the lowest. So far, there is no report on this characteristic. An explanation to this phenomenon is suggested. According to the mass balance equations[7], the averaged void fraction for slug flow can be described as

$$< \alpha_{SU} >= \frac{U_{SG} + < \alpha_{LS} > (U_{TB} - U_{GLS})}{U_{TB}} \quad (2)$$

Among the involved variables, U_{GLS} is constant and smaller than U_{TB}. Thus the average void fraction ($< \alpha_{SU} >$) is mainly influenced by U_{TB} and $< \alpha_{LS} >$. The variations of these two parameters in the developing process of slug flow are as follows:

(1) The liquid slugs formed in the entrance are very short, and the velocities of the Taylor bubbles (U_{TB}) behind the short slugs are fairly high[5]. During the developing process of the slug flow, most of liquid slugs will become longer, at the same time the average U_{TB} will decrease gradually. The decrease of U_{TB} leads to the increase of $< \alpha_{SU} >$.

(2) In the entrance, large quantity of gas exists in the liquid slugs in form of small bubbles by the action of turbulent dispersion. It leads to a higher value of $< \alpha_{LS} >$ in this zone. Along with the flow developing, the small bubbles will merge into the large bubbles, which makes $< \alpha_{LS} >$ decrease. At last $< \alpha_{LS} >$ will tend to be stabilized.

Therefore, the averaged void fraction at x = 80D is smaller than that of in the entrance (x = 30D) probably due to the decrease of $< \alpha_{LS} >$, and the averaged void fraction at x = 150D is higher than that of at x = 80D due to the decrease of U_{TB}.

4 LIQUID SLUG VOID FRACTION

4.1 Radial profiles

Figure 6 shows the radial profiles of void fraction in liquid slugs. Under all experimental conditions, the void fraction in the pipe central zone is relatively uniform. Away from the pipe centerline, the void fraction increases quickly to peak between 0.75R and 0.85R. Then, it decreases steeply and vanishes at the pipe wall. This kind of profile is similar to the experimental result of void fraction for the bubble flow reported by Serizawa *et al.*[8].

To sum up, the radial profile of liquid slug void fraction for vertical slug flow has the following characteristics: it is relatively uniform in the pipe central zone, but there is an obvious peak near the pipe wall. This is because the local liquid velocity across the pipe section is not uniform.

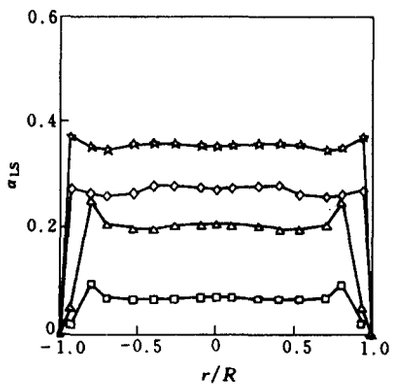

Figure 6 Radial distribution of liquid slug void fraction
($U_{SL} = 0.157\,m\cdot s^{-1}$, $x = 150D$)
U_{SG}, $m\cdot s^{-1}$: □ 0.287; △ 0.742; ◇ 1.196; ☆ 2.902

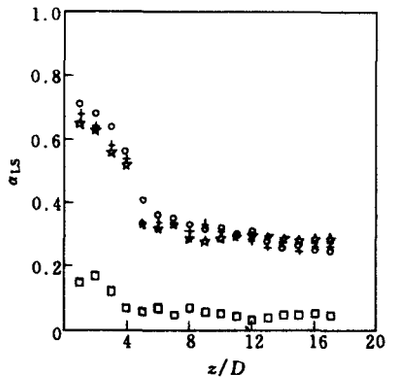

Figure 8 Axial void fraction distribution in the liquid slug at various radial positions
($U_{SL} = 0.157\,m\cdot s^{-1}$, $U_{SG} = 1.792\,m\cdot s^{-1}$, $x = 150D$)
r, m: ○ 0; + $0.53R$; ★ $0.80R$; □ $0.93R$

4.2 Axial void fraction distribution in liquid slugs at various radial positions

The axial void fraction distributions within the liquid slugs at various radial positions are depicted in Figs. 7 and 8. The axis z is from liquid slug head towards its tail. The variations of void fraction along the liquid slug are quite similar under the two experimental conditions in Figs. 7 and 8. The "wake region" and the "developed region" can be clearly recognized. Furthermore, in the zone of $z = 1D$, the highest value of void fraction can be found at all radial locations.

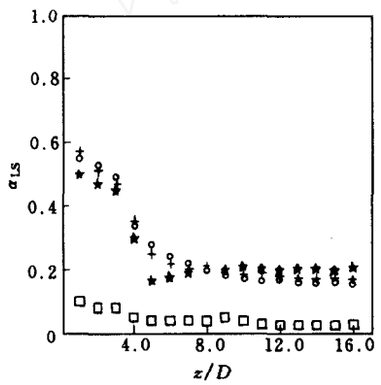

Figure 7 Axial void fraction distribution in the liquid slug at various radial positions
($U_{SL} = 0.157\,m\cdot s^{-1}$, $U_{SG} = 0.742\,m\cdot s^{-1}$, $x = 150D$)
r, m: ○ 0; + $0.53R$; ★ $0.80R$; □ $0.93R$

In the wake region, the void fraction measured at each radial location decreases steeply with z, and the maximum void fraction value turns up at the centerline. This demonstrates that the radial profile of liquid slug void fraction in the wake region is parabolic in shape.

In the developed region, the values of void fraction at each radial location are almost constant. When z is greater than $12D$, the maximum void fraction value at a given axial position turns up at the location of $r = 0.8R$. It implies that void fraction distribution for the fully developed liquid slug zone is of the saddle shape.

4.3 Averaged void fraction within liquid slug

The averaged void fraction within the liquid slug is an important parameter describing features of gas-liquid slug flow. Sylvester[3] proposed an empirical correlation as follows

$$< \alpha_{Ls} >= \frac{U_{SG}}{0.425 + 2.65(U_{SG} + U_{SL})} \qquad (3)$$

The comparison between liquid slug void fraction calculated by Eq. (3) and the current experimental data is shown in Fig. 9. The agreement can be observed within 20%.

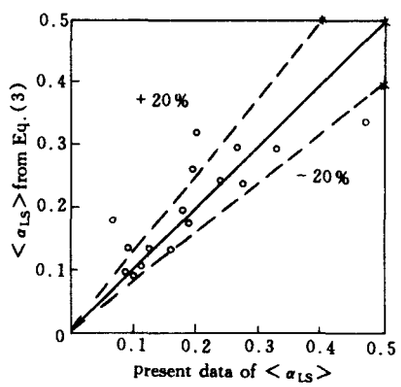

Figure 9 Comparison of liquid slug void fraction calculated by Eq. (3) with the experimental data
($x = 150D$)

4.4 Radial profiles of liquid slug void fraction at different axial locations

The radial profiles of liquid slug void fraction at different axial locations are represented in Fig. 10. Although there are the void fraction peaks close to the

wall, it is slightly different for the local void fraction values among the entrance ($30D$), the developing region ($80D$) and the fully developed region ($150D$). The peak value of void fraction at $80D$ is slightly less than that of at $150D$. The nearer is the measuring station from the entrance, the further is the peak location away from the wall. Moreover, the void fraction in the entrance is obviously higher around the centerline, which is due to the existence of big spherical cap bubbles. With the development of flow up to fully developed region, the profile curve becomes relatively flat around the centerline.

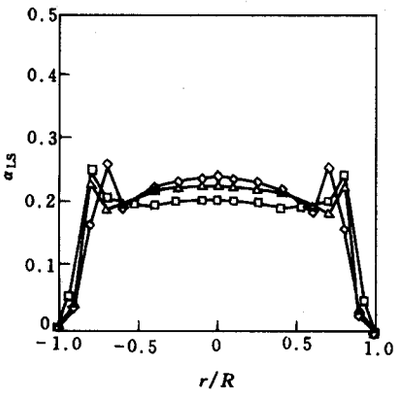

Figure 10 Radial profile of liquid slug void fraction at different axial locations
($U_{SL} = 0.157\,m\cdot s^{-1}$, $U_{SG} = 0.742\,m\cdot s^{-1}$)
○ $150D$; □ $80D$; △ $30D$

NOMENCLATURE

D	inside diameter, m
F	threshold value
L_{stab}	minimum stable slug length
R	radius, m
r	radial position, m
U	velocity, $m\cdot s^{-1}$
x	axial position, m
z	axial distance from the front of liquid slug, m
α	void fraction
$< >$	cross-sectional averaged value

Subscripts

G	gas phase
GLS	gas phase in liquid slug
LS	liquid slug
SG	superficial gas velocity
SL	superficial liquid velocity
SU	slug unit
TB	Taylor bubble

REFERENCES

1 Reinecke, N., Petritsch, G., Boddem, M., Mewes, D., "Tomographic imaging of the phase distribution in two-phase slug flow", *Int. J. Multiphase Flow*, **24**, 617—634 (1998).
2 Akagawa, K., Sakaguchi, T., "Fluctuation of void ratio in two-phase flow", *Bulletin of JSME*, **9** (33), 104—110 (1966).
3 Mao, Z. S., Dukler, A. E., "An experimental study of gas-liquid slug flow", *Exp. Fluids*, **8**, 169—182 (1989).
4 Van Hout, R., Shemer, L., Barnea, D., "Spatial distribution of void fraction within a liquid slug and some other related slug parameters", *Int. J. Multiphase Flow*, **18**, 831—845 (1992).
5 Xia, G. D., Zhou, F. D., Hu, M. S., "Liquid slug length distribution of gas-liquid two-phase slug flow in a vertical tube", *J. Chem. Eng. Ind. (China)*, **48** (6), 729—735 (1997). (in Chinese)
6 Taitel, Y., Barnea, D., "Two-phase slug flow", *Adv. Heat Transfer*, **20**, 83—132 (1990).
7 Xia, G. D., Li, S. X., Zhou, F. D., Hu, M. S., "A hydrodynamic model for gas-liquid slug flow in inclined tubes", *Progress in Natural Science*, **8**, 554—562 (1998).
8 Serizawa, A., Kataota, I., Michiyoshi, I., "Turbulence structure of bubbly flow—Local Properties", *Int. J. Multiphase Flow*, **12**, 235—246 (1975).
9 Sylvester, N. D., "A mechanistic model for two-phase vertical slug flow in pipes", *ASME J. Energy Resources Technology*, **109**, 206—213 (1987).